Journal of Imaging Science and Technology® 57(2): 020503-1–020503-5, 2013.

Local Structural Adaptive Total Variation Method for Image Restoration

Weili Zeng and Xiaobo Lu
School of Automation, Southeast University, Nanjing 210096, China
E-mail: xblu2013@126.com

Abstract. *In this article, a local structure adaptive total variation (LSATV) method for image restoration is presented. In our method, a discontinuity indicator is first proposed based on the eigenvalues of the structure tensor, which can effectively distinguish between edges and noises. Based on the proposed discontinuity indicator, a p norm is adaptively selected to match the local structure property of a pixel. Therefore, the proposed LSATV method inherits the advantages of both the Tikhonov regularization method and the total variation regularization method. Experimental results show the robustness of the proposed method and its superiority to state-of-the-art methods.*

[DOI: 10.2352/J.ImagingSci.Technol.2013.57.2.020503]

INTRODUCTION

The degradation of an image is usually unavoidable during formation, recording, and transmission, and it may affect latter processing, such as object detection and recognition. Therefore, image restoration forms a significant preliminary step in many computer vision tasks, and it has become a main research topic in the past few years.[1–3] It is well known that images are slightly noised or blurred during formation, recording and transmission process. So image restoration aims at deblurring and denoising the observed images.

A commonly used model is the following. Let $\Omega \subset \mathbb{R}^2$ be a bounded domain, let $u : \Omega \to \mathbb{R}$ be an original image describing the real scene, and let u_0 be the observed image of the same scene. The relationship between the observed image u_0 and the real image u is expressed by the following linear equation:

$$u_0 = Au + n, \tag{1}$$

where A is a blur operator and n is the additive noise.

The goal of image restoration is to recover the original image u from the observed image u_0. The restoration problem is ill conditioned since the degraded image u_0 and the real image u are typically related through a blur operator A. A widely used way to overcome the ill-posed minimization problem is to add a regularization term to the energy. One of the most widely referenced regularization methods for image restoration is the Tikhonov regularization method.[4] The authors proposed considering the following minimization problem:

$$E(u) = \frac{1}{2}\int_\Omega |u_0 - Au|^2 \mathrm{d}x + \frac{\lambda}{2}\int_\Omega |\nabla u|^2 \mathrm{d}x, \tag{2}$$

where the regularization parameter λ acts as a balancing factor between the fidelity and the smoothing term. The Euler–Lagrange equation for (2) in the gradient descent form is given by

$$\frac{\partial u}{\partial t} = (A^* u_0 - A^* A u) + \lambda \Delta u, \tag{3}$$

where A^* is the transpose of A. However, the noisy and edge pixels both contain high-frequency energy; the edges will be over-smoothed using the L_2 norm of the magnitude of the gradient.[5]

In Ref. 6, Rudin, Osher, and Fatemi proposed using total variation (TV) as the regularization term, which penalizes the total amount of change in the image as measured by the L_1 norm of the magnitude of the gradient. They proposed the following TV-based image restoration model:

$$E(u) = \frac{1}{2}\int_\Omega |u_0 - Au|^2 \mathrm{d}x + \frac{\lambda}{2}\int_\Omega |\nabla u| \mathrm{d}x. \tag{4}$$

It was designed with the explicit goal of preserving sharp edges in images while removing noise and other unwanted fine-scale details. The TV model has subsequently been extensively studied.[7–9] However, the TV method and its variances tend to cause a staircase effect in the processed image.[10,11] Recently, Fu and Zhang proposed an adaptive non-convex TV regularization for image restoration.[12] This model can preserve edges while removing noises, but this model uses the gradient as the discontinuity indicator, which cannot effectively distinguish between edges and isolated noises.

In order to overcome the disadvantage of the above work, in this article we present a local structure adaptive (LSA) TV model based on a discontinuity indicator for image restoration, which can effectively preserve edge information during noise removal. Experimental results show the effectiveness of the proposed method.

The remainder of this article is organized as follows. The section given below proposes the local structure adaptive TV (LSATV) restoration model. Numerical experiments are presented in the section 'Experimental results' and the article is concluded in the final section.

Received May 1, 2012; accepted for publication May 22, 2013; published online Mar. 1, 2013. Associate Editor: Wei Koh.
1062-3701/2013/57(2)/020503/5/$20.00

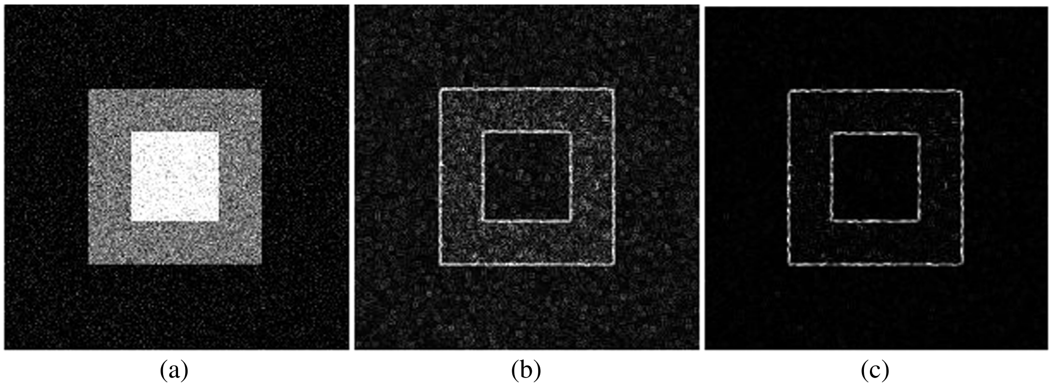

Figure 1. Comparison effects on a noisy image. (a) Noisy image, (b) effect of the gradient, and (c) effect of the proposed discontinuity indicator.

LOCAL STRUCTURE ADAPTIVE TV RESTORATION MODEL

The adaptive selection of the p norm plays a very important role in the restoration process. However, as shown in the introduction, state-of-the-art methods select the p norm based on the image gradient as the discontinuity indicator, which cannot effectively distinguish between edges or textures and noises. Therefore, we first propose a new discontinuity indicator based on the eigenvalues of the structure tensor, and then define the p norm based on the proposed discontinuity indicator.

It is well known that the structure tensor can preserve local structure information than gradient.[13] Therefore, we use it to perform local structure information analysis. The structure tensor matrix is defined as $J_0 = \nabla u \cdot \nabla u^T$, where ∇u denotes the gradient image of u. In order to incorporate the neighboring structural information, the structure tensor is then computed by convolution of the components of J_0 with a Gaussian kernel

$$J_\sigma = G_\sigma * (\nabla u \cdot \nabla u^T), \tag{5}$$

where G_σ denotes a Gaussian kernel with a standard deviation σ.

Denote by $\lambda_{\min}$ and $\lambda_{\max}$ the minimum and maximum eigenvalues of J_σ, respectively. Define the discontinuity indicator as

$$\gamma = \lambda_{\max} - \lambda_{\min}.$$

For a pixel (x, y) in a smooth region, $\lambda_{\max}(x, y)$ and $\lambda_{\min}(x, y)$ are both small, so $\gamma(x, y)$ is small; for a pixel (x, y) in an edge region, $\lambda_{\max}(x, y)$ is large and $\lambda_{\min}(x, y)$ is small, so $\gamma(x, y)$ is large; for an isolated noise (x, y), $\lambda_{\max}(x, y)$ and $\lambda_{\min}(x, y)$ are both large, so γ is small. According to the above analysis, edges can be distinguished from smooth regions and isolated noise based on the value of γ. Figure 1 shows the comparison of the effects on a noisy image between the image gradient and the proposed discontinuity indicator. It can be seen that our proposed discontinuity indicator γ can effectively distinguish between edges and noises, but the discontinuity indicator based on the image gradient does not work effectively in the noisy image.

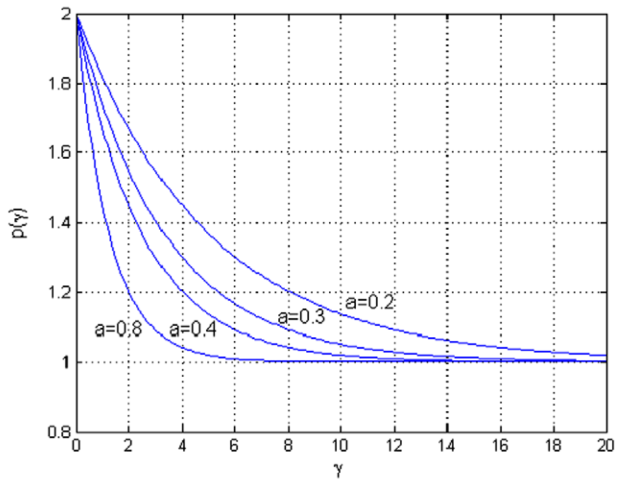

Figure 2. $p(\gamma)$ for different values of a ($a = 0.2, 0.3, 0.4, 0.8$).

Therefore, using the proposed discontinuity indicator would appear to be a good way in which to improve the TV model. The LSATV model is proposed as follows:

$$E(u) = \int_\Omega \frac{1}{p(\gamma)} |\nabla u|^{p(\gamma)} \mathrm{d}x + \frac{\lambda}{2} \int_\Omega |u_0 - Au|^2 \mathrm{d}x, \tag{6}$$

where the function $p(\gamma)$ is defined as

$$p(\gamma) = 1 + \exp(-a\gamma), \tag{7}$$

where a is a constant. Figure 2 shows $p(\gamma)$ for different values of a. Note that $p(\gamma)$ is a monotonically decreasing function from 2 to 1. For smooth regions and isolated noise, $\gamma \to 0$, so $p(\gamma) \to 2$. At edges or textures, $\gamma \to \infty$, so $p(\gamma) \to 1$. Therefore, the p norm is adaptively determined.

The Euler–Lagrange equation associated to problem (6) is

$$\operatorname{div}\left(\frac{p(\gamma)\nabla u}{|\nabla u|^{2-p(\gamma)}}\right) + \lambda\left[A^T * (u_0 - A * u)\right] = 0. \tag{8}$$

We approximate the solution of (8) by means of the steepest gradient descent method, formulated as the

Table I. PSNR and SSIM performance comparison of "License plate" image.

Assessment method	$p = 1$	$p = 1.5$	$p = 2$	$p(\gamma)$
ISNR	3.6752	3.4528	3.2006	4.5437
SSIM	0.6857	0.6410	0.6119	0.7455

following partial differential equation:

$$\frac{\partial u}{\partial t} = \mathrm{div}\left(\frac{p(\gamma)\nabla u}{|\nabla u|^{2-p(\gamma)}}\right) + \lambda[A^T * (u_0 - A * u)]. \quad (9)$$

However, model (9) is relatively slow in reaching its steady state, and is also stiff, since the parabolic term is close to singular for small gradients, which is similar to the TV model.[14] In order to guarantee the stability of (9), an ad hoc rule of thumb indicates that the time step ∇t and the space step size ∇x need to be related by[7]

$$\frac{\nabla t}{\nabla x^2} \leqslant l\left|\nabla^2 u\right|$$

for fixed $l > 0$. This Courant–Friedrichs–Lewy (CFL) restriction is what we shall relax. This issue was seen in numerical experiments. In order to accelerate the evolution procedure, we multiply the right-hand side of (9) by $|\nabla u|^{2-p(\gamma)}$:

$$\frac{\partial u}{\partial t} = |\nabla u|^{2-p(\gamma)}\mathrm{div}\left(\frac{p(\gamma)\nabla u}{|\nabla u|^{2-p(\gamma)}}\right) + \lambda|\nabla u|^{2-p(\gamma)}[A^T * (u_0 - A * u)]. \quad (10)$$

Note that Eq. (9) is not well defined at points where $\nabla u = 0$, because of the presence of the term $1/|\nabla u|^{2-p(\gamma)}$. Therefore, from the analytical point of view, the solution of Eq. (10) approaches the same steady state as the solution of Eq. (9) whenever u has nonzero gradient. Below, we test the convergence speed of model (9) and model (10).

In terms of explicit partial derivatives, model (10) can be expressed as

$$\frac{\mathrm{d}u}{\mathrm{d}t} = \lambda(u_x^2 + u_y^2)^{1-\frac{p(\gamma)}{2}}[A^T * (u_0 - A * u)] + \frac{(p(\gamma)-1)u_x^2 u_{xx} + u_{xx}u_y^2 - (4-2p(\gamma))u_x u_y u_{xy} + (p(\gamma)-1)u_y^2 u_{yy} + u_{yy}u_x^2}{u_x^2 + u_y^2}, \quad (11)$$

with homogeneous Neumann boundary conditions and u_0 as initial guess.

We construct an explicit discrete scheme to numerically solve differential equation (11). Let $u_{i,j}^n$ be the approximation to an $N \times M$ sized image $u(x_1, x_2, t_n)$, where $x_1 = 0, 1, \ldots, M-1$ and $x_2 = 0, 1, \ldots, N-1$. In order to compute the right hand size of (11), we denote by

$$\nabla_x^+ u_{i,j}^n = u_{i+1,j}^n - u_{i,j}^n, \quad \nabla_x^- u_{i,j}^n = u_{i-1,j}^n - u_{i,j}^n,$$
$$\nabla_y^+ u_{i,j}^n = u_{i,j+1}^n - u_{i,j}^n, \quad \nabla_y^- u_{i,j}^n = u_{i,j-1}^n - u_{i,j}^n.$$

We define the discrete derivative terms as[15]

$$[u_{xx}]_{i,j}^n = \nabla_x^+\nabla_x^- u_{i,j}^n/h^2, \quad [u_{yy}]_{i,j}^n = \nabla_y^+\nabla_y^- u_{i,j}^n/h^2,$$
$$[u_{xy}]_{i,j}^n = (\nabla_x^+ + \nabla_x^- u_{i,j}^n)(\nabla_y^+ + \nabla_y^- u_{i,j}^n)/4h^2$$
$$\left[\frac{\mathrm{d}u}{\mathrm{d}t}\right]_{i,j}^n = \frac{u_{i,j}^n - u_{i,j}^{n-1}}{\delta t}, \quad [u_x]_{i,j}^n = (\nabla_x^+ + \nabla_x^-)u_{i,j}^n/2h,$$
$$[u_y]_{i,j}^n = (\nabla_y^+ + \nabla_y^-)u_{i,j}^n/2h.$$

These derivatives are computed using a symmetric boundary. The normalized step difference energy (NSDE) is used to measure the convergence.[16] The NSDE is defined as

$$\mathrm{NSDE} = \frac{|u^n - u^{n-1}|^2}{|u^{n-1}|^2},$$

where u^n and u^{n-1} denote, respectively, the image vector at the nth iteration and at the $n-1$th iteration.

EXPERIMENTAL RESULTS

In this section, we test the proposed method on the "License plate" image with size 171×157 and the "Barbara" image with size 256×256 (taken from the USC-SIPI image database). These two images are shown in Figure 3(a) and Figure 5(a), respectively. The performance of the method is evaluated by measuring the improvement in the signal to noise ratio (ISNR) and the structural similarity (SSIM).[17] A trial-and-error method is used to pick the optimal parameters, and the best result is chosen as the output of the method.

The ISNR is defined as

$$\mathrm{ISNR} = 10 \cdot \log 10\left(\frac{\sum_{i,j}[u(i,j) - u_0(i,j)]^2}{\sum_{i,j}[u(i,j) - u_r(i,j)]^2}\right), \quad (12)$$

where $u_0(\cdot)$ is the initial image (noised and blurred image) and $u_r(\cdot)$ is the restored image. The larger the value of the ISNR, the better the restored image.

The SSIM is defined as

$$\mathrm{SSIM} = \frac{(2\mu_{u_0}\mu_{u_r} + C_1)(2\sigma_{u_0} + C_2)}{(\mu_{u_0}^2 + \mu_{u_r}^2 + C_1)(\sigma_{u_0}^2 + \sigma_{u_r}^2 + C_2)}, \quad (13)$$

where μ_{u_0} and μ_{u_r} are the mean intensity of the initial image u_0 and the mean intensity of the restored image u_r, respectively. σ_{u_0} and σ_{u_r} are the standard deviation of the initial image u_0 and the standard deviation of the restored image u_r, respectively. C_1 and C_2 are two positive constants.

We first study the effects of the p norm. We consider the noisy and blurry image in Fig. 3(b) generated by first convolving the original "License plate" image with a Gaussian kernel (5×5 mask, $\sigma = 1$) and then adding Gaussian white noise with variance 25. The ISNR and SSIM values of the different methods are presented in Table I. In Fig. 3(c)–(f), we list the restored "License plate" image with $p = 1$ (TV method),[9] $p = 1.5$, $p = 2$ (Tikhonov method),[4] and the proposed LSATV method, respectively. It can be seen that Tikhonov method ($p = 2$) can over-smooth the image and that the TV method ($p = 1$) tends to cause a staircase

Figure 3. Comparison of results on "License plate". (a) Original image, (b) noisy and blurry image, (c) $p = 2$ (Tikhonov method), (d) $p = 1.5$, (e) $p = 1$ (TV method), (f) LSATV method ($\lambda = 0.2$, $a = 0.1$).

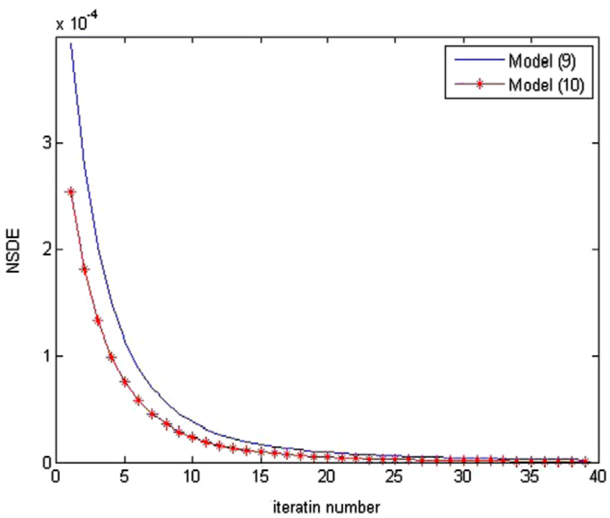

Figure 4. Normalized step difference energy for model (9) and model (10).

effect in the processed image. The proposed LSATV method obtains better ISNR and SSIM, and better visual effects.

Next, we designed an evaluation of the convergence performance of model (9) and (10). Figure 4 shows a plot of the NSDE for model (9) and model (10). It is seen that the convergence speed of model (10) is better than that of model (9). Moreover, the results from model (10) is stable and similar to that of model (9).

Finally, we compare the proposed LSATV method with the ATV method.[12] The essential difference between two methods is the selection of the p norm. In Fig. 5(a)–(b), we show the "Barbara" image and the corresponding noisy and blurry image generated by convolving a Gaussian kernel (3×3 mask, $\sigma = 1$) adding Gaussian white noise with variance $\sigma = 20$, respectively. Fig. 5(c)–(d) show restored images obtained by using the ATV method and the LSATV method, respectively. Clearly, the proposed LSATV method shows better results than the ATV method. In the non-smooth region, the edge structure information, especially the fine edge, is better preserved. In the smooth region, the noise is removed effectively.

CONCLUSIONS

In this article, a local structure adaptive total variation (LSATV) method for image restoration is proposed, which inherits the advantages of both the Tikhonov regularization method and the TV regularization method. The proposed method first presents a discontinuity indicator based on the eigenvalues of the structure tensor, and then the p norm is adaptively selected based on the proposed discontinuity indicator. Experimental results show the effectiveness of the proposed method. It is important to emphasize that the proposed model can effectively preserve edges during noise removal, so it may be a new idea for image superresolution.[18]

ACKNOWLEDGMENTS

The authors would like to thank the editor and the anonymous reviewers for their suggestions. This work was supported by National Natural Science Foundation of China (60972001), the National Key Technologies R&D Program of China (2009BAG13A06), the Scientific Innovation Research of College Graduate in Jiangsu Province (CXZZ_0163), and

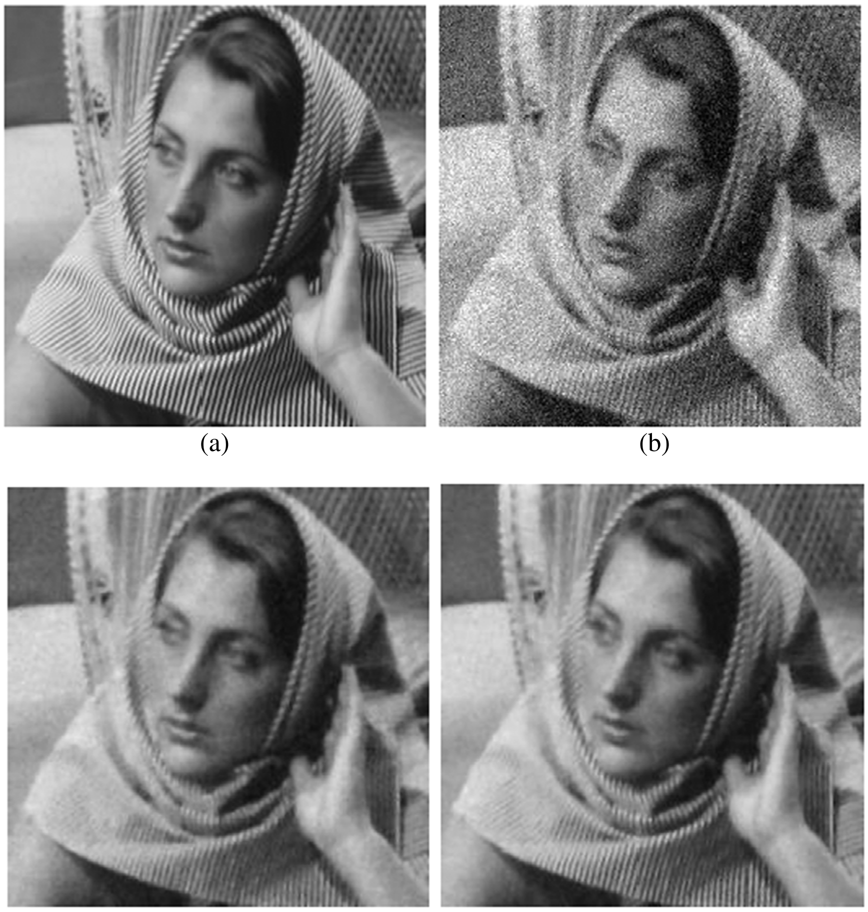

(a) (b) (c) (d)

Figure 5. Comparison of results between the ATV and LSATV methods on "Barbara". (a) Original image, (b) noisy and blurry image, (c) ATV method, (d) LSATV method ($\lambda = 0.1$, $a = 0.05$).

the Scientific Research Foundation of the Graduate School of Southeast University (YBPY1212).

REFERENCES

[1] M. E. Celebi, H. A. Kingravi, B. Uddin, and Y. A. Asl, "Fast switching filter for impulsive noise removal from color images," J. Imag. Sci. Technol. **51**, 155–165 (2007).

[2] S. Kalaivani and R. S. D. Wahidabanu, "Diagnostic ultrasound image enhancement: a multiscale permutation approach," J. Imag. Sci. Technol. **56**, (2012) 10501-1-10501-12.

[3] W. Zeng and X. Lu, "Region-based non-local means algorithm for noise removal," Electron. Lett. **47**, 1125–1127 (2011).

[4] A. Tikhonov and V. Arsenin, *Solutions of Ill-posed Problems* (Winston & Sons Inc, Washington, DC, 1977).

[5] L. Rudin and S. Osher, "Total variation based image restoration with free local constraints", *Proc. IEEE Internat. Conf. Imag. Proc.* (1994) pp. 31–35.

[6] L. Rudin, S. Osher, and E. Fatemi, "Nonlinear total variation based noise removal algorithm," Physica D **60**, 259–268 (1992).

[7] A. Marquina and S. Osher, "Explicit algorithms for a new time dependent model based on level set motion for nonlinear deblurring and noise removal," SIAM J. Sci. Comput. **22**, 387–405 (2000).

[8] Y. Chen, S. Levine, and M. Rao, "Variable exponent, linear growth functionals in image restoration," SIAM J. Appl. Math. **66**, 1383–1406 (2006).

[9] M. Lysaker and X. Tai, "Iteration image restoration combing total variational minimization and a second-order functional," Int J. Comput. Vis. **66**, 5–18 (2006).

[10] T. Chan, S. Esedoglu, F. Park, and A. Yip, *Recent Developments in Total Variation Image Restoration* (Springer, New York, USA, 2005).

[11] Y. L. You and M. Kaveh, "Fourth order partial differential equations for noise removal," IEEE Trans. Image Process. **9**, 1723–1730 (2000).

[12] S. Fu and C. Zhang, "Adaptive non-convex total variation regularization for image restoration," Electron. Lett. **46**, 907–908 (2010).

[13] T. Brox, J. Weickert, B. Burgeth, and P. Mrazek, "Nonlinear structure tensors," Image and Vision Comput. **24**, 41–55 (2006).

[14] W. Zeng and X. Lu, "A robust variational approach to super-resolution with nonlocal TV regularization term," Imaging Sci. J. **61**, 268–278 (2013).

[15] Y. Cao, J. Yin, Q. Liu, and M. Li, "A class of nonlinear parabolic–hyperbolic equations applied to image restoration," Nonlinear Anal. Real World Appl. **11**, 253–261 (2010).

[16] S. H. Lee and J. K. Seo, "Noise removal with Gauss curvature-driven diffusion," IEEE Trans. Image Process. **14**, 126–136 (2005).

[17] Z. Wang, A. Bovik, and H. Sheikh, "Image quality assessment: from error visibility to structural similarity," IEEE Trans. Image Process. **13**, 600–612 (2004).

[18] W. Zeng and X. Lu, "A generalized DAMRF image modeling for super-resolution of license plates," IEEE Trans. Intelli. Transp. Syst. **13**, 828–837 (2012).